LBL-12599

CONF-810862--1

Lawrence Berkeley Laboratory
UNIVERSITY OF CALIFORNIA

ENERGY & ENVIRONMENT
DIVISION

To be presented at the Illuminating Engineering Society Annual Technical Conference, Toronto, Canada, August 9-13, 1981

DAYLIGHTING CALCULATIONS FOR NON-RECTANGULAR INTERIOR SPACES WITH SHADING DEVICES

Michael F. Modest

June 1981

Prepared for the U.S. Department of Energy under Contract W-7405-ENG-48

DISCLAIMER

LBL-12599
EEB-W-81-05
W-81

Paper to be presented at the Illuminating Engineering Society (IES) Annual Technical Conference, Toronto, Canada, August 9-13, 1981.

DAYLIGHTING CALCULATIONS FOR NON-RECTANGULAR INTERIOR SPACES WITH SHADING DEVICES

Michael F. Modest*

Lawrence Berkeley Laboratory
University of California
Berkeley CA 94720

*Department of Mechanical Engineering
University of Southern California
University Park
Los Angeles, California 90007

JUNE 1981

The work described in this paper was supported by the Assistant Secretary for Conservation and Solar Energy, Office of Buildings and Community Systems, Buildings Division of the U.S. Department of Energy under Contract No. W-7405-ENG-48.

This manuscript was printed from originals provided by the author.

ABSTRACT

Employing a general numerical model described in an earlier paper, the sensitivity of daylighting to nonrectangular rooms, such as L-shaped rooms, and to other internal visual obstructions, such as light-shelves, is discussed. In addition, the model has been expanded to allow the treatment of opaque, semi-transparent and translucent window overhangs, which may be positioned at any or all sides of a window. Further, the model has now the capability of graphical output. Thus, all results are shown in the form of contour plots, showing room outline, sunny areas, and constant-illumination or constant-daylight factor lines.

INTRODUCTION

Prediction of daylight illumination levels in a room are, by necessity, subject to a compromise between accuracy and numerical complexity. If only crude knowledge of general illumination levels is needed, simple models, such as the one by Bryan [1], which do not require use of a digital computer, may be sufficient. For more accurate evaluations the code developed by DiLaura et al. [2-5] represents the state of the art, at the expense of substantial computer time requirements. Nevertheless, even the sophisticated model by DiLaura et al. is subject to a number of confining restrictions: (i) only rectangular rooms with horizontal and vertical rectangular surfaces can be modeled; (ii) the room may not have any internal obstructions; (iii) internal reflections as well as window overhangs are modeled in a very approximate fashion. The above shortcomings are dictated by the need to keep computational time within reasonable bounds. It should be kept in mind here that DiLaura's is a general lighting code, of which daylighting is only one element. A new model was recently introduced by Modest [6], addressing specifically the problem of daylighting, which relaxes the three confining restrictions mentioned above. In his latest paper DiLaura [7] describes how rectangular visual obstructions could be incorporated into his model. The present paper describes usage and further development of the model given in [6].

Three items are addressed in detail:

(1) The sensitivity of daylighting to non-rectangular rooms is

discussed. The rooms may be non-rectangular in nature without internal visual obstructions, such as A-frames with triangular windows, etc. On the other hand, non-rectangular rooms may be composed of rectangular surfaces, but have visual obstructors, such as L-shaped rooms, etc.

(2) The treatment of opaque, semi-transparent and translucent window overhangs and their effects on daylighting is discussed. The overhangs are assumed to be of rectangular shape and may be located above, below, and/or to the sides of a window.

(3) To date all models [2-6] result in output of tabular form, while the architectural user would prefer graphical representation. The present model incorporates an interpolation and plotting package which displays results graphically, including

(a) room shape, size and orientation; weather conditions, etc.

(b) window location and size;

(c) light-level contours on a working surface, either showing lines of constant illumination, or lines of constant daylight factor;

(d) contours of sunny areas on the working surface, if any.

It is anticipated that the present model will give the illuminating engineer and architect new insight into the science of daylighting of non-standard spaces. The model should prove a valuable research tool in the future.

Many aspects of the present model, such as geometric description, evaluation procedures for luminances, etc., have been discussed in

detail in Ref. [6]. We will repeat here the description of geometric modeling for the convenience of the reader and give a brief outline of how luminances are obtained.

GEOMETRIC MODELING OF INSIDE AND OUTSIDE SURFACES

The inside of the room is assumed to consist of N plane surfaces of trapezoidal shape (see Figure 1). This is considered to be adequately general to model any present room design of practical importance. These N surfaces comprise N_c clear windows, N_{sc} clear windows with sheer curtains, N_d diffusing windows, and N_w opaque walls, which reflect light diffusely. Clear windows are understood to be surfaces that partially transmit light without directional scattering. Diffuse (or translucent) windows, on the other hand, are assumed to scatter transmitted light equally into all directions (milky-texture glass, windows with shades, etc.). Sheer-curtain windows are assumed to partially transmit light directly, and to partially diffuse the light (dirty windows, fly screens, sheer-curtained windows, etc.). Each of the opaque surfaces may have other surfaces as cut-outs, e.g. windows, large dark pictures, etc.

Location and dimensions of each surface are described by a local coordinate system which is then related to an overall stationary coordinate system. The local coordinate system (see Figure 1) has its origin located so that the X'-axis runs along one of the two parallel

sides of the trapezoid. The z'-axis is chosen so that it points perpendicularly into the room.

The overall stationary coordinate system is chosen in the following manner:

(i) arbitrary fixed origin,

(ii) x-axis pointing from origin towards south,

(iii) y-axis pointing from origin towards east,

(iv) z-axis pointing from origin vertically into the sky (zenith).

To totally describe a surface "i" the local coordinate syystem must be related to the overall coordinate system. To accomplish this the following data are required:

(i) location (X_{oi}, Y_{oi}, Z_{oi}) of the local coordinate system's origin with respect to the overall origin,

(ii) β_{xi} and β_{yi}, that is, the polar angles formed by the x'- and y'-axes with respect to the absolute z-axis,

(iii) ψ_{xi} and ψ_{yi}, that is, the azimuth angles of the x'- and y'-axes in the x-y plane (the angles between the x-axis and the projection of the x'- or y'-axis),

(iv) X_{1i}, X_{2i}, X_{3i}, and Y_i, that is, characteristic dimensions of surface "i" as depicted in Figure 1,

(v) if the surface is a window, its thickness, that is, the width of the hole through which light can penetrate (d_i).

The overall coordinates of any point (x',y') on a surface A_i can then be described by the equations

$$\begin{aligned} x_i &= X_{oi} + \ell^i_{11}\, x' + \ell^i_{12}\, y' , \\ y_i &= Y_{oi} + \ell^i_{21}\, x' + \ell^i_{22}\, y' , \\ z_i &= Z_{oi} + \ell^i_{31}\, x' + \ell^i_{32}\, y' , \end{aligned} \tag{1}$$

which are subject to the restrictions,

$$\begin{aligned} \frac{X_{2i}}{Y_i}\, y' \le x' \le X_{1i} - \frac{X_{1i} - X_{3i}}{Y_i}\, y' , \\ 0 \le y' \le Y_i . \end{aligned} \tag{2}$$

The values ℓ^i_{mn} in Eq. (1) are the direction cosines between the m-axis of the overall system and the n-axis of the local system. They are computed from the following equations:

$$\begin{aligned} \ell^i_{11} &= \hat{i} \cdot \hat{i}_i = \sin\beta_{xi} \cos\psi_{xi} , \\ \ell^i_{21} &= \hat{j} \cdot \hat{i}_i = \sin\beta_{xi} \sin\psi_{xi} , \\ \ell^i_{31} &= \hat{k} \cdot \hat{i}_i = \cos\beta_{xi} , \\ \ell^i_{12} &= \hat{i} \cdot \hat{j}_i = \sin\beta_{yi} \cos\psi_{yi} , \\ \ell^i_{22} &= \hat{j} \cdot \hat{j}_i = \sin\beta_{yi} \sin\psi_{yi} , \\ \ell^i_{32} &= \hat{k} \cdot \hat{j}_i = \cos\beta_{yi} , \\ \ell^i_{13} &= \hat{i} \cdot \hat{k}_i = \sin\beta_{xi} \sin\psi_{xi} \cos\beta_{yi} - \cos\beta_{xi} \sin\beta_{yi} \sin\psi_{yi} , \\ \ell^i_{23} &= \hat{j} \cdot \hat{k}_i = \cos\beta_{xi} \sin\beta_{yi} \cos\psi_{yi} - \sin\beta_{xi} \cos\psi_{xi} \cos\beta_{yi} , \\ \ell^i_{33} &= \hat{k} \cdot \hat{k}_i = \sin\beta_{xi} \sin\beta_{yi} \sin(\psi_{yi} - \psi_{xi}) . \end{aligned} \tag{3}$$

Equations (1) and (2) may be rewritten in nondimensional

coordinates

$$\eta = \frac{y'}{y_i} \; ; \quad \xi = \frac{x' - x_{2i}\eta}{x_{1i} - (x_{1i} - x_{3i} + x_{2i})\eta} \quad , \tag{4}$$

such that

$$\begin{aligned} x_i &= x_{oi} + \ell^i_{11}\,[x_{1i} - (x_{1i} - x_{3i} + x_{2i})\eta]\xi + (\ell^i_{11}\,x_{2i} + \ell^i_{12}\,y_i)\eta \;, \\ y_i &= y_{oi} + \ell^i_{21}\,[x_{1i} - (x_{1i} - x_{3i} + x_{2i})\eta]\xi + (\ell^i_{21}\,x_{2i} + \ell^i_{22}\,y_i)\eta \;, \\ z_i &= z_{oi} + \ell^i_{31}\,[x_{1i} - (x_{1i} - x_{3i} + x_{2i})\eta]\xi + (\ell^i_{31}\,x_{2i} + \ell^i_{32}\,y_i)\eta \;, \end{aligned} \tag{5}$$

restricted by

$$0 \le \eta \le 1, \quad 0 \le \xi \le 1. \tag{6}$$

An "enclosure" is assigned to each window in the room (unless the window is a skylight which sees only the sky). Windows that are cutouts located in the same wall may view the same enclosure. All surfaces in the outside enclosure are assumed to be plane and of trapezoidal shape as is the case for inside surfaces. For outside surfaces, no cutouts are allowed (for example, a building facade with windows is assigned an overall reflectivity), and all surfaces are either diffuse and opaque or part of the sky. The surfaces in the enclosure are described in the same manner as those inside the room, that is, each surface is assigned a local coordinate system and that system is then related to the overall coordinate system. Thus, Figure 1 and Eqs. (1) through (6) hold for both inside and outside surfaces.

DETERMINATION OF THE LUMINANCE DISTRIBUTION ON EXTERNAL AND INTERNAL SURFACES

For simplicity it is assumed that each outside surface has a constant (average) luminance over its entire surface area, with the exception of differentiating between sunny and shady areas. Light exchange factors between outside surfaces and the sky or other outside surfaces are determined by the Monte Carlo method, in which a statistical sample of light bundles is traced. This method ensures adequate accuracy (as compared to the modeling of the outsides by simple configurations) combined with small computational effort (since only a relatively small sample is required). Once the light exchange factors are known, the outside luminances are evaluated by matrix inversion of the simultaneous equations describing outside luminances [6].

Inside the room luminances may not only vary significantly across the surfaces, but this variation may also profoundly affect the illumination on the working surface. It is, therefore, necessary to break up inside surfaces into a number of subsurfaces or nodes. While a light balance again results in a number of simultaneous equations for nodal luminances, the inside case is different from the outside case in two respects: (i) because of the large number of nodes (typically 40 to 200 per surface) matrix inversion becomes impractical; luminances are, therefore, found through iterations (depending on surface reflectivities 2 to 3 iterations usually prove sufficient); (ii) again because of the large number of nodes, the nodes are usually sufficiently small and far apart, so that the light exchange factors may be evaluated from a simple

algebraic formula [6].

INTERNAL VISUAL OBSTRUCTIONS

As indicated earlier, the present model allows the treatment of visual obstructions inside the room, such as non-rectangular rooms (e.g. L-shaped rooms, Fig. 2), light shelves (see Fig. 3), or furniture (desks, bookshelves, etc.), as long as all surfaces can be constructed from trapezoidal shapes. As indicated by DiLaura [7] the numerical effort of treating obstructions will become prohibitive if straight-forward finite-differencing is used in a room with many nodes. The computational effort has been reduced considerably by applying the following considerations. First, as part of the input of the computer program, an obstruction identifier is given for each pair of surfaces. Consider, for example, the L-shaped room in Fig. 2. Sidewall (3) can "see" sidewall (5), or floor (8), etc., without any visual obstructions in between. On the other hand, its view of sidewall (7), or floor (9), is partially obstructed by sidewall (5) (but no other surface!). Thus, in the calculation of light exchange factors, visual obstructions must be considered only in a few cases. If an obstruction is possible, the exchange factor between nodal area A_{ik} on surface i and nodal area A_{jl} on surface j is determined by

$$F_{ik\to j\ell} \simeq \left[\delta(A_{ik}-A_{j\ell})\,\frac{\cos\beta_{ij}\,\cos\beta_{ji}}{\pi\,S_{ij}^{2}}\right]_{avg.} A_{j\ell}\;;\quad \frac{A_{ik}A_{j\ell}}{S_{ij}^{4}} < 1\;. \tag{7}$$

Here S_{ij} is the distance between the two nodes, and the β are the angles between the ray and the surface normals to surfaces i and j, respectively. The δ-function is equal to unity if there is no visual obstruction between the nodes, and zero if there is. The value of δ is determined by finding the intersection of the unit vector $\hat{r}$, pointing from node A_{ik} to A_{jl},

$$\hat{r} = [(x_{j\ell} - x_{ik})\hat{i} + (y_{j\ell} - y_{ik})\hat{j} + (z_{j\ell} - z_{ik})\hat{k}]/S_{ij}, \tag{8}$$

on the plane in which the obstructing surface A_q lies. If $\vec{r}_{ik}$ is the vector pointing from the overall origin to A_{ik}, and $\vec{r}_q$ is the vector pointing to the point of intersection on the obstructing plane, then

$$\frac{(\vec{r}_q - \vec{r}_i)\cdot\hat{i}_q}{\hat{r}\cdot\hat{i}_q} = \frac{(\vec{r}_q - \vec{r}_i)\cdot\hat{j}_q}{\hat{r}\cdot\hat{j}_q} = \frac{(\vec{r}_q - \vec{r}_i)\cdot\hat{k}_q}{\hat{r}\cdot\hat{k}_q} \tag{9}$$

From this the point of intersection is determined in local q-plane coordinates as

$$x_q' = [x_{ik} - X_{oq} + a(x_{j\ell} - x_{ik})]\ell_{11}^q + [y_{ik} - Y_{oq} + a(y_{j\ell} - y_{ik})]\ell_{21}^q + [z_{ik} - Z_{oq} + a(z_{j\ell} - z_{ik})]\ell_{31}^q \tag{10}$$

$$y_q' = [x_{ik} - X_{oq} + a(x_{j\ell} - x_{ik})]\ell_{12}^q + [y_{ik} - Y_{oq} + a(y_{j\ell} - y_{ik})]\ell_{22}^q + [z_{ik} - Z_{oq} + a(z_{j\ell} - z_{ik})]\ell_{32}^q \tag{11}$$

where

$$a = \frac{(x_{ik} - X_{oq})\ell_{13}^{q} + (y_{ik} - Y_{oq})\ell_{23}^{q} + (z_{ik} - Z_{oq})\ell_{33}^{q}}{(x_{ik} - x_{j\ell})\ell_{13}^{q} + (y_{ik} - y_{j\ell})\ell_{23}^{q} + (z_{ik} - z_{j\ell})\ell_{33}^{q}} \qquad (12)$$

The restriction given by Eq. (2) is now applied to determined whether (x_q, y_q) is actually within the bounds of the obstructing surface.

In summary, for each nodal pair that may have one or more obstructions between them, Eqs. (10) to (12) must be evaluated. However, the calculations consist of only a few multiplications, and have to be performed only for a limited number of surface pairs due to the introduction of obstruction identifiers, thus preserving numerical efficiency.

MODELING OF WINDOW OVERHANGS

If a window is shielded by opaque, semi-transparent or translucent overhangs (on any or all of its sides), this may have a strong regulatory effect on the light distribution within the room. Consequently, the light reflected from or transmitted through the overhangs must be determined in order to predict illumination distribution accurately. It will be assumed in the present model that overhangs may be positioned to the top of, to the sides of, and to the

bottom of each window. Each overhang is assumed to be rectangular and of width w; the base of each overhang, which is perpendicular to the window, is parallel to the perimeter of the window at a distance d_o (see Fig. 3). Thus, if the size and location of the window is known in vector form, the vector equations describing the four possible overhangs are easily derived (not reproduced here). The luminances of the overhangs' inside surfaces (i.e., the surfaces "seen" by the window), are readily determined if one assumes that the overhangs do not influence significantly the luminance distribution in the surroundings. In that case the light exchange factors with sky and surroundings are again conveniently calculated by the Monte Carlo method after the luminances of other outside surfaces have been determined.

GRAPHICAL DISPLAY OF RESULTS

In order to get a good grasp of the light distribution within an enclosure, a graphical display of results is vastly preferable over tabular display for most architectural users. The present plotting routine is designed to produce a graphical display of illumination or daylight-factor results, including the following features:

(i) a printout of weather data (sky condition, sun position, outside horizontal illumination);

(ii) a drawing of the working surface(s), with attached axes showing units of length;

(iii) outlines of the window positions;

(iv) a windrose showing the orientation of the working surface(s);

(v) outline of sunny areas on the working surface(s) if present;

(vi) contour lines on the working surface(s) showing constant levels of illumination or daylight factors; and

(vii) a table identifying the contour levels.

At the present time, the graphics package is only able to treat rectangular working surfaces. However, this limitation applies only to the working surfaces; any wall, window, etc., may be of trapezoidal shape.

In order to position the plot, a local coordinate system for the plot must be defined. This has been chosen to be identical to the local coordinate system used for the description of working surface No. 1. Thus the corner of working surface No. 1, that has been chosen as the local origin, will become the lower left-hand corner of the plot. Keeping this in mind, the user may arrange the plot to his or her liking. All other locations on the plot, such as size and location of other working surfaces, location of windows, size shape and locations of sunny areas, etc.., are expressed in terms of this coordinate system. This is achieved by first applying Eqs. (1), i.e. by finding the overall coordinates for any given points, and then applying the inverse of Eq. (1), i.e.

$$\vec{r}_i = \vec{r} - \vec{R}_i, \tag{13}$$

where $\vec{r}_i$ is the vector pointing to the point under consideration in the plot-coordinate system (first working surface local coordinate system), $\vec{r}$ is the vector pointing to that point from the origin of the overall coordinate system, and $\vec{R}$ is the vector pointing to the origin of the local system. Thus

$$\begin{aligned} x_i &= (x-X_{0i})\ell^i_{11} + (y-Y_{0i})\ell^i_{21} + (z-Z_{0i})\ell^i_{31}; \\ y_i &= (x-X_{0i})\ell^i_{12} + (y-Y_{0i})\ell^i_{22} + (z-Z_{0i})\ell^i_{32}. \end{aligned} \tag{14}$$

Finding the image of sunny areas on the working surfaces is somewhat more involved, as allowance has to be made for the width of the window wall. One must find the image of the inside of the window opening as well as the image of the outside opening onto the working surfaces. The overlap between these two areas represents the area illuminated directly by the sun. This is achieved in a number of steps (see Fig. 5):

(i) The image of the inside opening is found by calculating its four corner points x_{fi}, y_{fi}, $i = 1,4$.

(ii) The image for the outside opening is calculated as x_{bi}, y_{bi}, $i = 1,4$.

(iii) Tracing rays from the inside corners of the window towards the sun, one finds that only one actually goes through the outside opening; let this point be $i = j$. The coordinates (x_{fj}, y_{fj}) represent a corner of

the actual sun image.

(iv) Similarily the point $(x_{b,j+2}, y_{b,j+2})$ represents another corner of the sun image.

(v) The other two points are found by finding the intersections between the straight lines forming the image, i.e.

$$y = y_{f,j} + (y_{f,j\pm1} - y_{f,j})(x - x_{f,j})/(x_{f,j\pm1} - x_{f,j})$$
$$= y_{b,j+2} + (y_{b,j+2\pm1} - y_{b,j+2})(x - x_{b,j+2})/(x_{b,j+2\pm1} - x_{b,j+2}) \quad (15)$$

In the above relations it was assumed that subscripts were corrected to $j \leftarrow \text{mod}(j,4)$ (e.g. if $j = 6$, j is changed to $j = 6 - 4 = 2$).

There are presently three different plotting options to represent the array of illumination and daylight-factor data:

Option 1: Plots lines of constant illumination, spaced fairly evenly apart. The actual levels plotted depend on the maximum illumination, I_{max} encountered:

	Levels plotted (in foot-candles)
$I_{max} \leq$ 200 f-c	5, 10, 15, 20, 25, 37.5, 50, 62.5, 75, 100, 125. . . . .
200 < $I_{max} \leq$ 400 f-c	10, 20, 30, 40, 50, 75, 100, 125, 150, 200, 250. . . . .
400 < I_{max}	20, 40, 60, 80, 100, 150, 200, 250, 300, 400, 500. . . . .

Option 2: Plots lines of constant illumination; levels are chosen as constant steps in foot-candles:

	Levels plotted (in foot-candles)
$I_{max} \leq$ 300 f-c	10, 20, 30, 40, 50 . . . . .
I_{max} > 300 f-c	20, 40, 60, 80, 100. . . . .

Option 3: Plots lines of constant daylight factor; levels are chosen as 1/2%, 1%, 2%, 3%, 4%,. . .

To plot the lines of constant illumination or daylight factor, respectively, a standard interpolation computer routine is employed, which was modified to suit the present purpose. The most important modification is due to the fact that the standard computer routine is limited to rectangular surfaces. In order to allow more than one working surface (L-shaped rooms, etc.), a search routine had to be generated to locate adjacent data points on different working surfaces. Incorporating such adjacent data points into the interpolation scheme ensures smooth transitions of the constant-level lines from one working surface to the other.

DISCUSSION OF SAMPLE RESULTS

To demonstrate the power of the present model, and to illustrate the influence of window overhangs and of internal obstructions on daylight distribution, three different designs are considered in the following. In the first example an L-shaped room is considered as shown in Fig. 2, i.e. a room where some walls are partially obstructed from one another. In the seecond and third examples only the left rectangular half of the room ($y > 0$) is used, i.e. a solid side wall is introduced along the dashed line at $y = 0$. Example 2 looks at the effect of a light-shelf as shown in Fig. 3. The third example on the other hand, is concerned with the effects of window overhangs on the daylighting in such room. Design details for all three rooms are

summarized in Table 1.

Figure 6 shows lines of equal illumination onto a working surface in the L-shaped room on an overcast day. The working surface is 2.5 ft. above the floor, or at the height of the window sills. The plotted illumination levels are computer chosen as outlined in the last section. Comparing the light levels close to windows, one notices that there is less illumination close to the curtained window in the top half of the graph (due to the lower transmissivity) but more evenly distributed (due to the diffusing effect of sheer curtains). Near the curtained window light levels continue to rise all the way to the window, at the clear window they do not: this is due to the fact that, near the clear window, light from the sky travels at very shallow angles through the window to the working surface, at which the transmissivity is low. As the working surface had to be split into two parts, the light levels are plotted independently in the upper square and the lower rectangle. The accuracy of the interpolation scheme is seen by the slight discontinuities of the lines across the working surface separation.

Figure 7 shows the same room and conditions as in Fig. 6; however, here lines of equal daylight factors are plotted to demonstrate the versatility of the plotting routine. In all the following graphs only illumination levels, such as in Fig. 6, will be shown.

Figure 8 again shows the L-shaped room, but this time for a clear day with sun shining through the windows. In order to show smooth

contours of reasonable light levels, direct sunshine is excluded in the generation of constant illumination lines. Therefore, direct sunshine should be added to the amount of illumination shown within the crosshatched areas. This amounts to 4,534 foot-candles for clear window, and 1763 foot-candles for the sheer curtain window (these numbers are arrived at by multiplying 6,000 foot-candles of direct sun by the directional transmissivity and, in the case of the diffusing window, by the clearness factor). It is seen that, for a clear day, the light levels are higher close to the curtained window because of the large contribution of direct sunlight that has been diffused by the sheer curtain.

Figure 9 is identical to Fig. 6 without the 10' x 10' part of the L-shaped room and its window. The room is orientated differently in the plot (rotated by 90^{o}); this is due to the fact that for simple rooms (only rectangular surfaces and no internal visual obstructions) a simplified imput routine is used with the computer choosing plot-layout. Illumination lines in Figs. 6 and 9 differ from one another somewhat due to two different reasons: (i) light levels in Fig. 6 are generally a little higher due to the presence of the second window, which also produces slightly asymmetric curves, and (ii) lines in Fig. 6 are more accurate than in Fig. 9 as more data points were used for line generation (12 x 6 = 72 nodes for Fig. 6, and only 8 x 4 = 32 nodes for Fig. 9), in particular in regions of large illumination gradients (i.e. close to the window).

The influence of overhangs on the light levels in a similar room under similar sky conditions is shown in Figs. 10-13. Figure 10 is identical to Fig. 9, but an opaque overhang 7 ft. by 3 ft. in size is positioned 1 ft. above the window. The overhang reduces light levels close to the window considerably, but has only a minor effect in the back of the room (note that light level increments in Fig. 9 are different from the ones in Figs. 10 through 13). If a 3 ft. wide overhang is positioned on all four sides of the window (Fig. 11), the area close to the window becomes still darker, with the rest of the room relatively unaffected. In Fig. 12 the overhang is made of semitransparent material, while in Fig. 12 it is made of translucent material (top overhang only, nothing on sides and bottom). Again, the influence is felt only near the window with light-levels everywhere close to the no-overhang case. The translucent overhang darkens the room somewhat more than the semi-transparent one: due to its diffusing nature some of the transmitted sky-illumination is scattered into the surroundings rather than through the window.

Finally, in Figs. 14 through 19 the influence of another type of internal visual obstruction, viz. a light shelf as shown in Fig. 3, is demonstrated. Figure 14 shows the same basic 10 ft. x 20 ft. room on an overcast day. However the central 5 ft. x 5 ft. window is now replaced by a 10 ft. long window which occupies the top 3 ft. of the front wall over its entire width. Figs. 15 and 16 show the same room under the same conditions, but with a 4 ft. wide light shelf added which has a reflectivity of 90% and 20% respectively. The influence of the light

shelf and its reflectivity is seen to be dramatic (the strange shape of line #3 in Fig. 15 is due to slight inaccuracies close to corners combined with the fact that only 8 x 4 = 32 data points were used). The light shelf clearly demonstrates one desired effect, namely its ability to create large areas of nearly constant light levels.

Figures 17 through 19 are the equivalent to the last three figures, but for a clear sky. There is no sunny patch in Figs. 18 and 19 since the light shelf keeps the sun from reaching the working surface directly. Again the light shelf is seen to level out differences in illumination: without the light shelf illumination levels vary by approximately 550 foot-candles, which is reduced to c. 140 foot-candles and c. 40 foot-candles, respectively, for the high and low reflectivity shelves. The light shelf also tends to make illumination levels more or less symmetric.

ACKNOWLEDGEMENT

The work described in this paper was supported by the Assistant Secretary for Conservation and Renewable Energy, Office of Buildings and Community Systems, Buildings Division of the U. S. Department of Energy under Contract No. W-7405-ENG-48.

REFERENCES

1. H. J. Bryan, "A Simplified Procedure for Calculating the Effects of Daylight from Clear Skies," J. Illuminating Engineering Society, Vol. 9, pp. 142-151, 1980.

2. D. L. DiLaura, "On the Computation of Equivalent Sphere Illumination," J. Illuminating Engineering Society, Vol. 4, pp. 129-149, 1975.

3. D. L. DiLaura, "On the Computation of Visual Comfort Probability," J. Illuminating Engineering Society, Vol. 5, pp. 207-217, 1976.

4. D. L. DiLaura and G. A. Hauser, "On Calculating the Effects of Daylighting in Interior Spaces," J. Illuminating Engineering Society, Vol. 7, pp. 2-14, 1978.

5. D. L. DiLaura, "On a New Technique for Interreflected Component Calculations," J. Illuminating Engineering Society, Vol. 8, pp. 53-59, 1979.

6. M. F. Modest, "A General Model for the Calculation of Daylighting in Interior Spaces," to appear in Energy and Building, 1981.

7. D. L. DiLaura, "On Radiative Transfer Calculations in Unempty Rooms," J. Illuminating Engineering Society, Vol. 10, pp. 120-126, 1981.

Table 1: Design Data for Sample Rooms

Window number and size (1) L-shaped room	2 5 ft. x 5 ft. windows in south wall, centers 5 ft. above floor, 1 window with sheer curtain (α = .5)
(2) Rectangular room with light shelf	1 10 ft. x 3 ft. window in south wall, filling the top 3 ft. of window wall
(3) Rectangular room with overhangs	1 5 ft. x 5 ft. window as for (1)
Floor height above ground	30 ft
Window transmissivities (perpendicular to windows)	90%
Reflectivities: floor ceiling sidewalls	20% 70% 60%
Room height	10 ft.
Window wall thickness	1 ft.
Special features (1)	none
(2)	horizontal light shelf 10 ft. x 4 ft. below window perpendicular to window wall
(3)	overhangs on all four sides of window; perpendicular to window wall, 1 ft. away from window, 3 ft. wide
Object building and Surroundings	Room in center of 60 ft. x 30 ft. x 50 ft. building. Windows in 60 ft. E-W wall exposed to the South; identical opposing building to the North, with 50 ft. between buildings

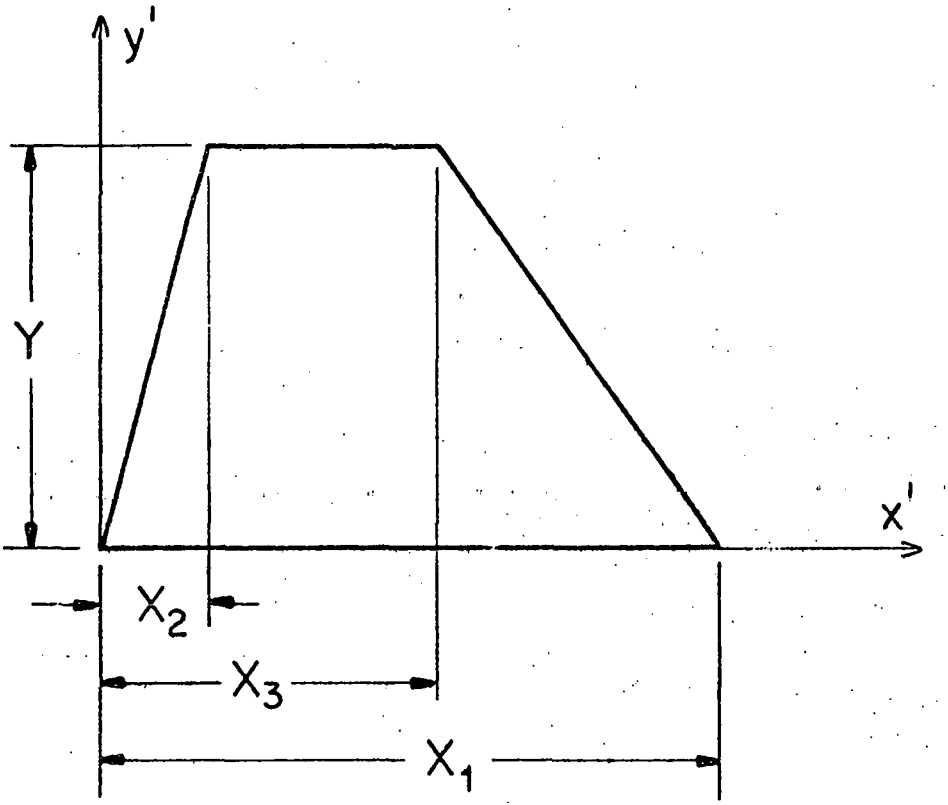

Fig. 1 Geometry of Allowable Surfaces

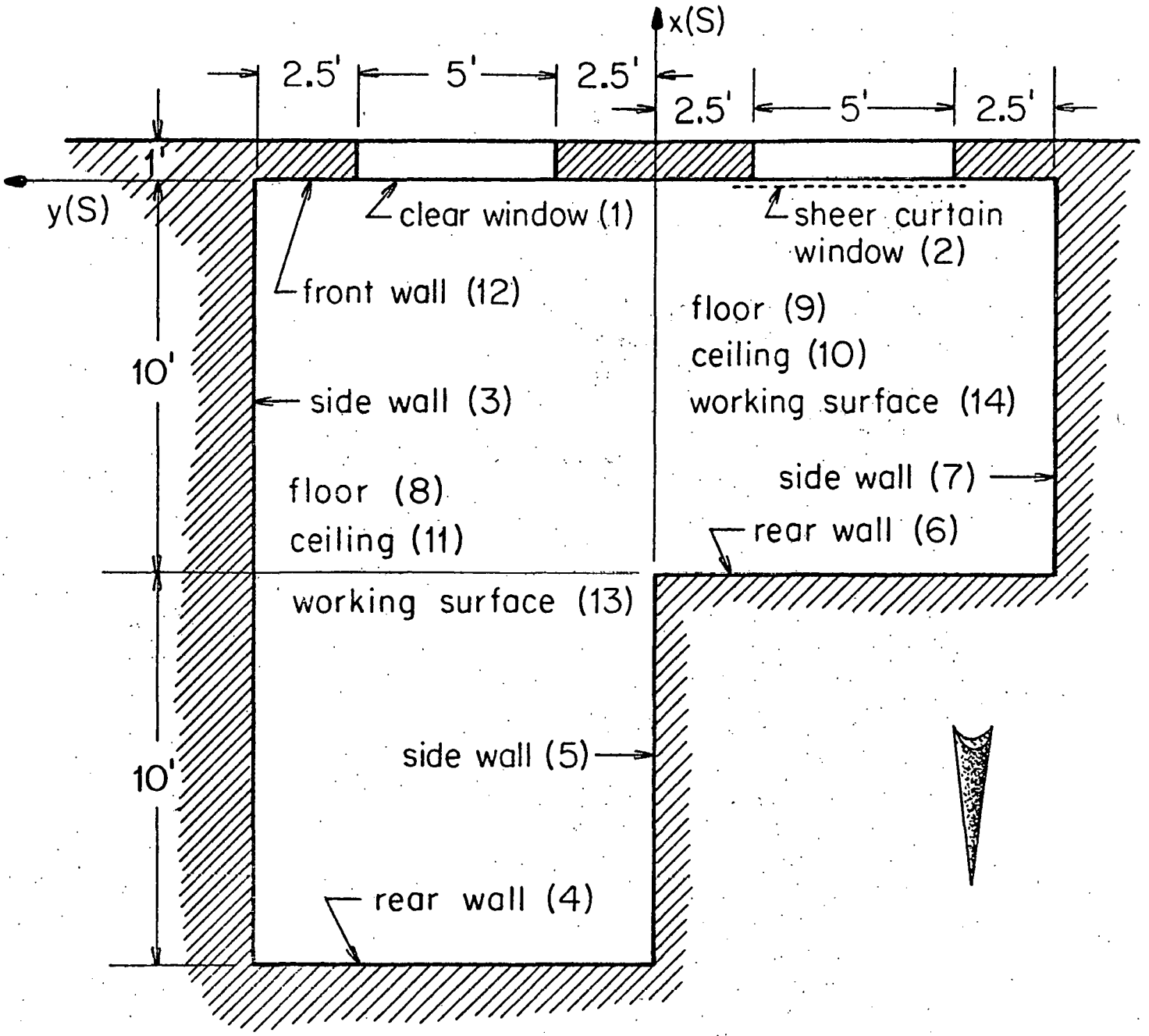

Fig. 2 Floor Plan of L-Shaped Room

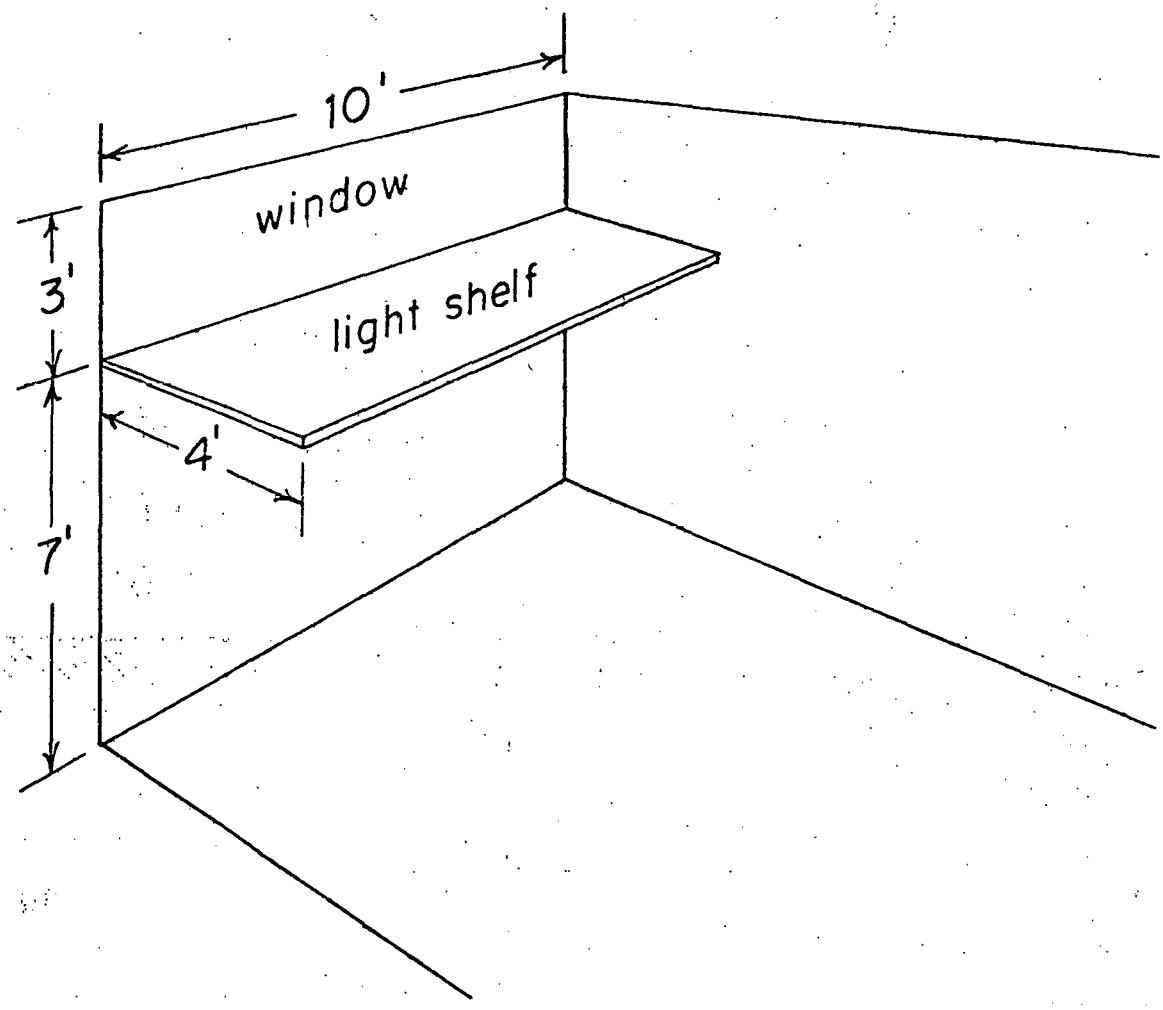

Fig. 3 Schematic for a Room With Light Shelf

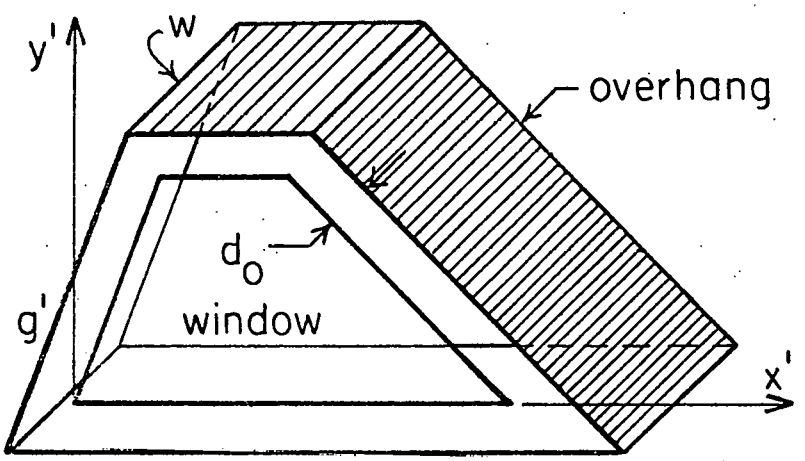

Fig. 4 Geometry of Window Overhangs

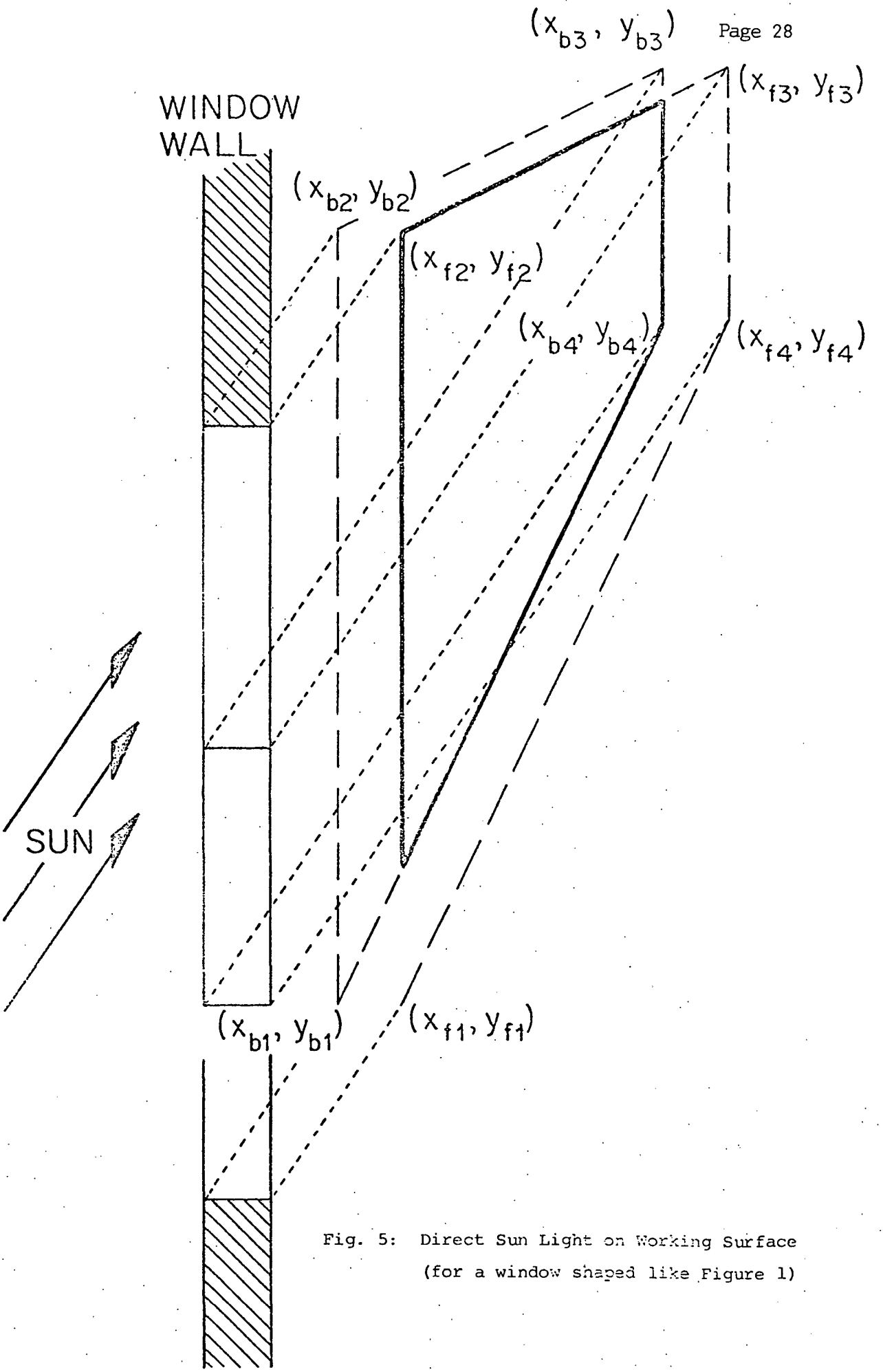

Fig. 5: Direct Sun Light on Working Surface
(for a window shaped like Figure 1)

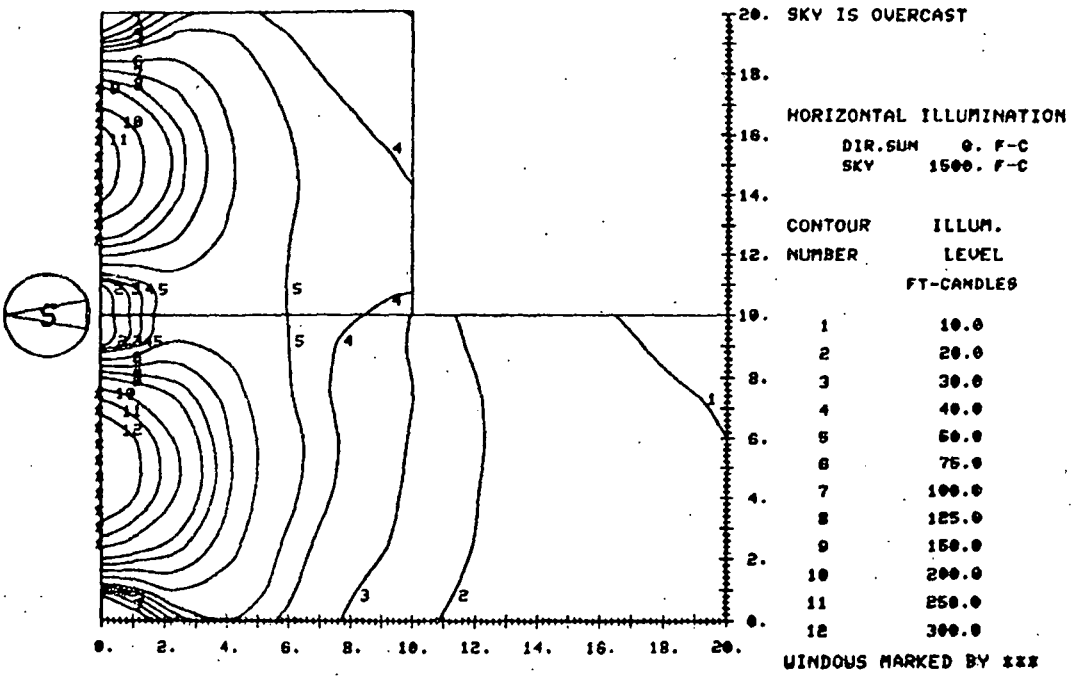

Figure 6: Illumination Levels in an L-shaped Room on an Overcast Day

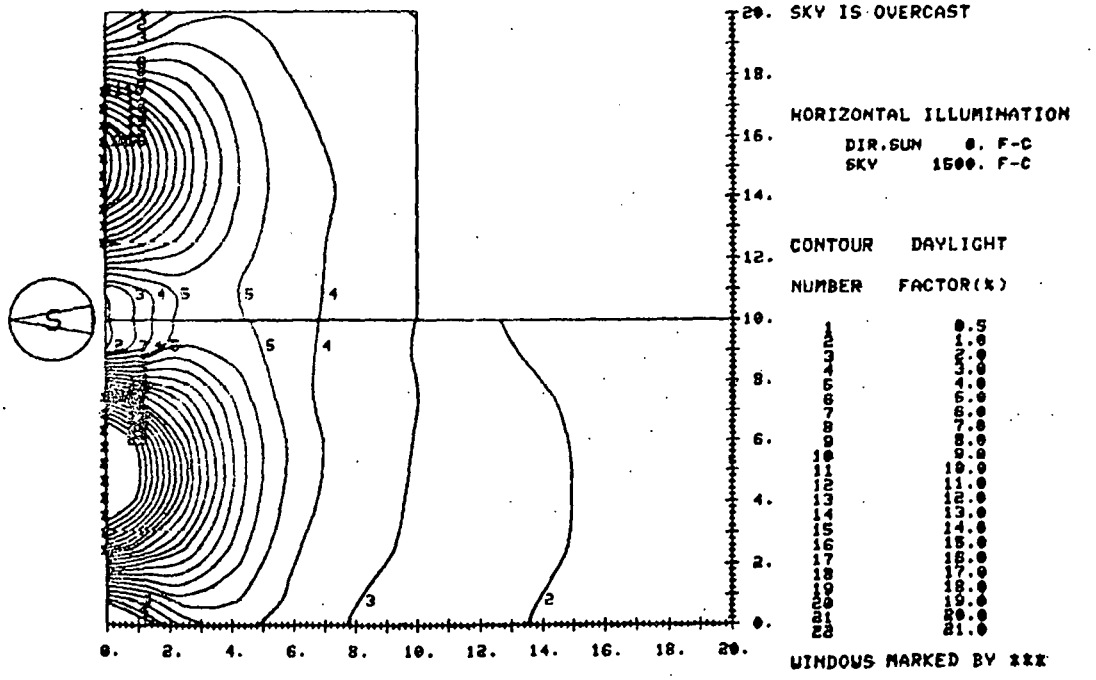

Figure 7: Daylight Factor Levels in an L-shaped Room on an Overcast Day

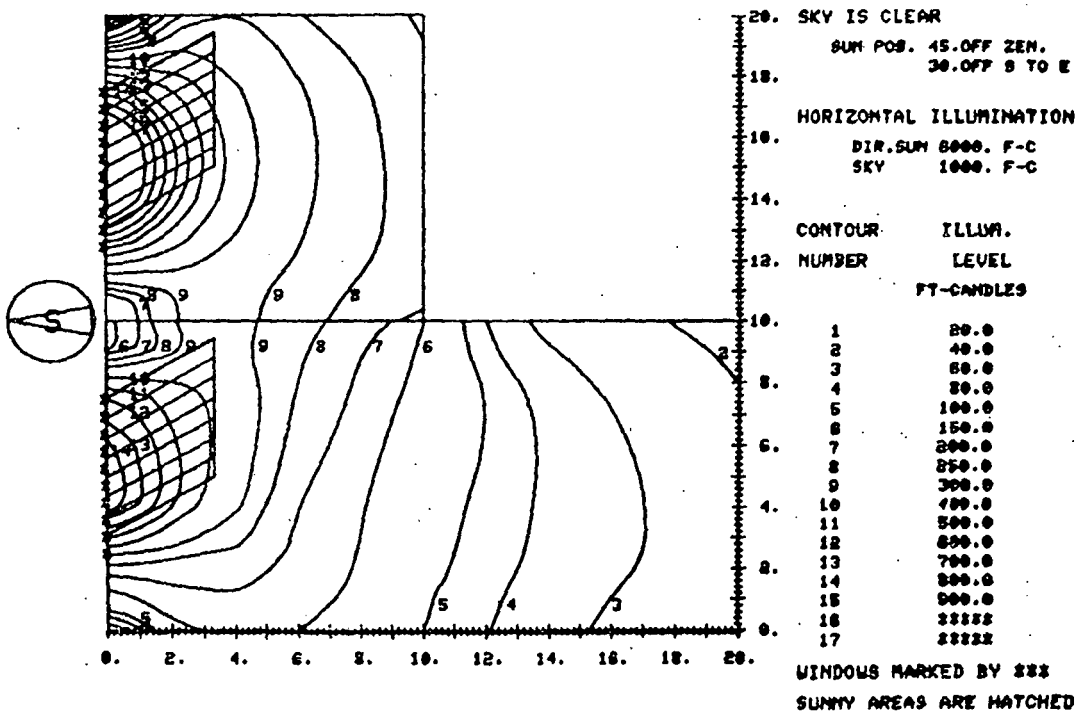

Figure 8: Illumination Levels in an L-shaped Room on a Clear Day

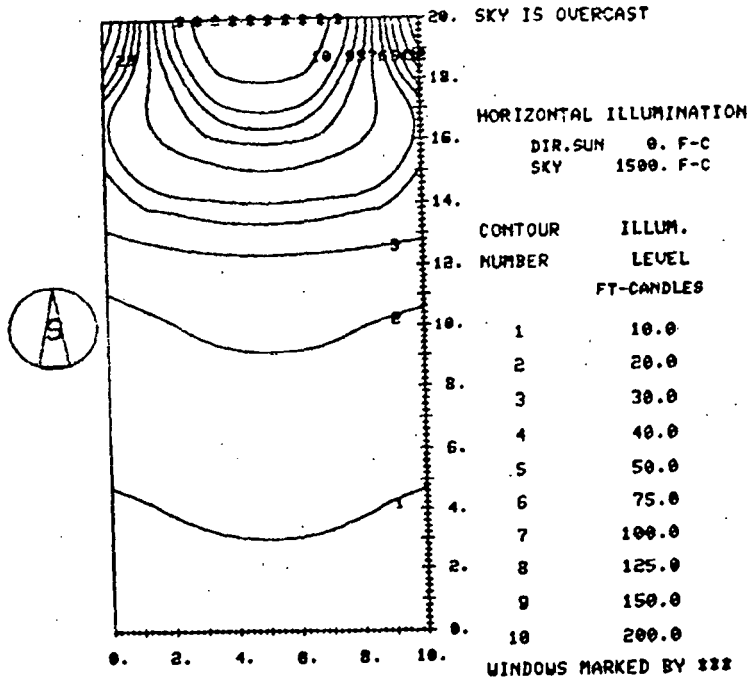

Figure 9: Illumination Levels in a Rectangular Room on an Overcast Day Without Window Overhang

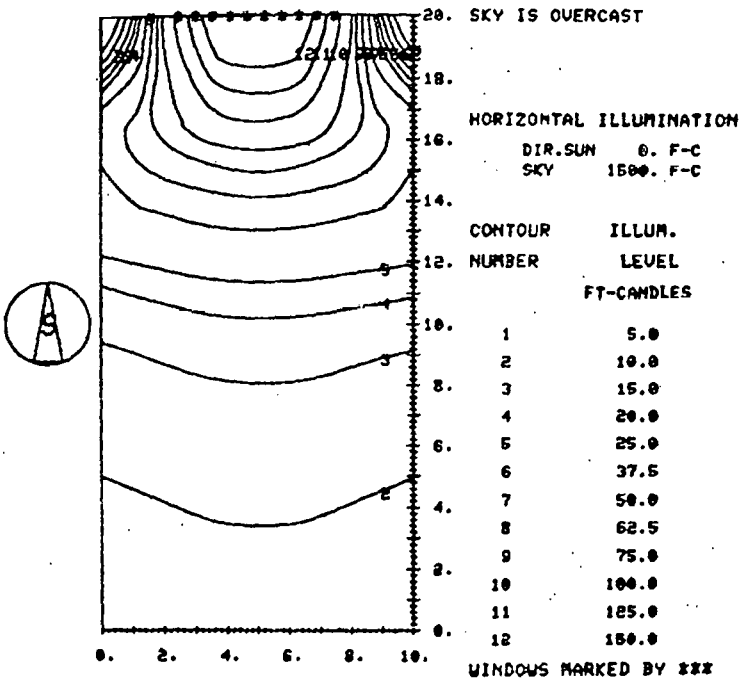

Figure 10: Illumination Levels in a Rectangular Room on an Overcast Day with Opaque Overhang on Top

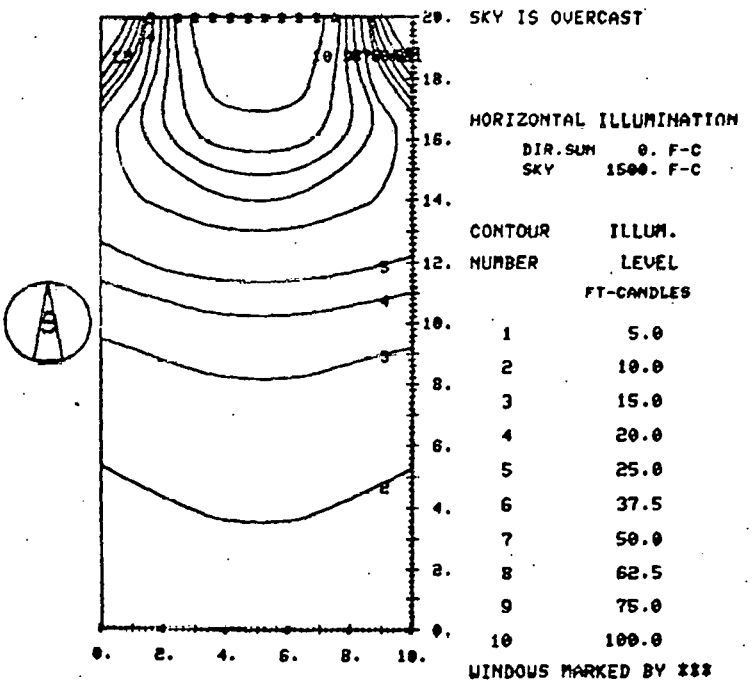

Figure 11: Illumination Levels in a Rectangular Room on an Overcast Day with Opaque Overhangs on All Four Sides

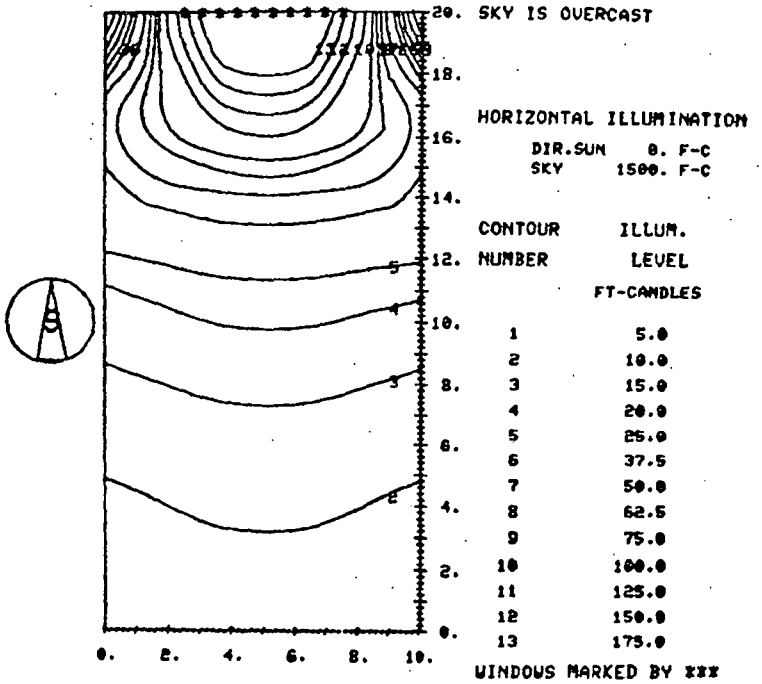

Figure 12: Illumination Levels in a Rectangular Room on an Overcast Day with Semi-Transparent Overhang on Top

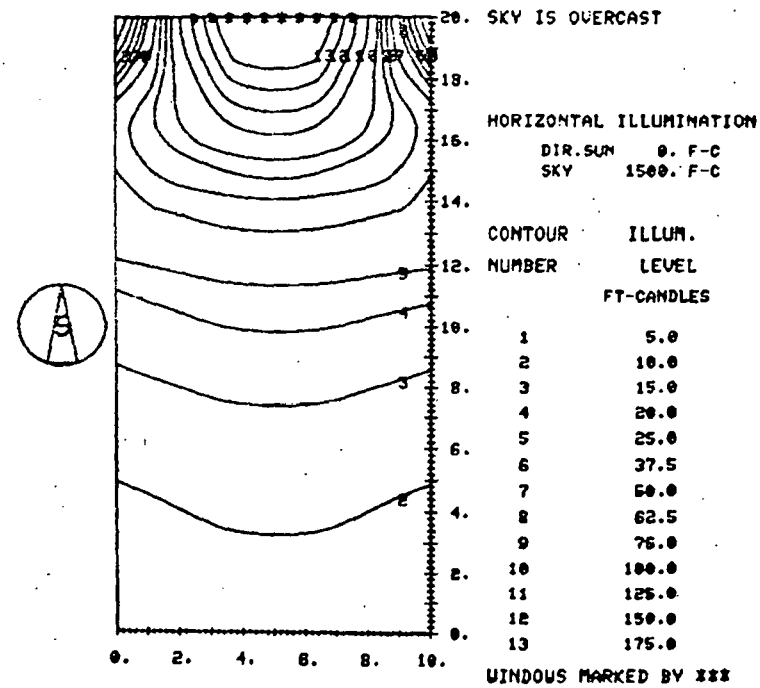

Figure 13: Illumination Levels in a Rectangular Room on an Overcast Day with Translucent Overhang on Top

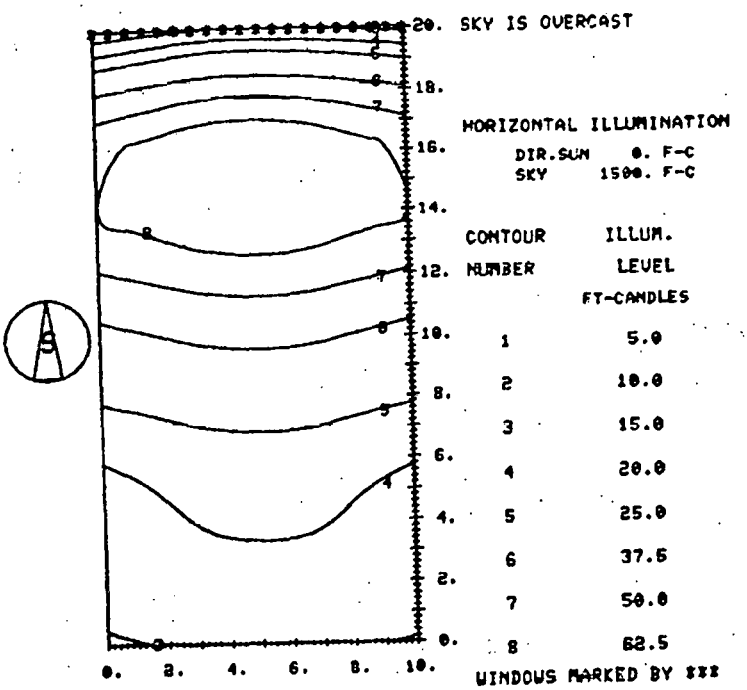

Figure 14: Illumination Levels in a Rectangular Room on an Overcast Day Without Light Shelf

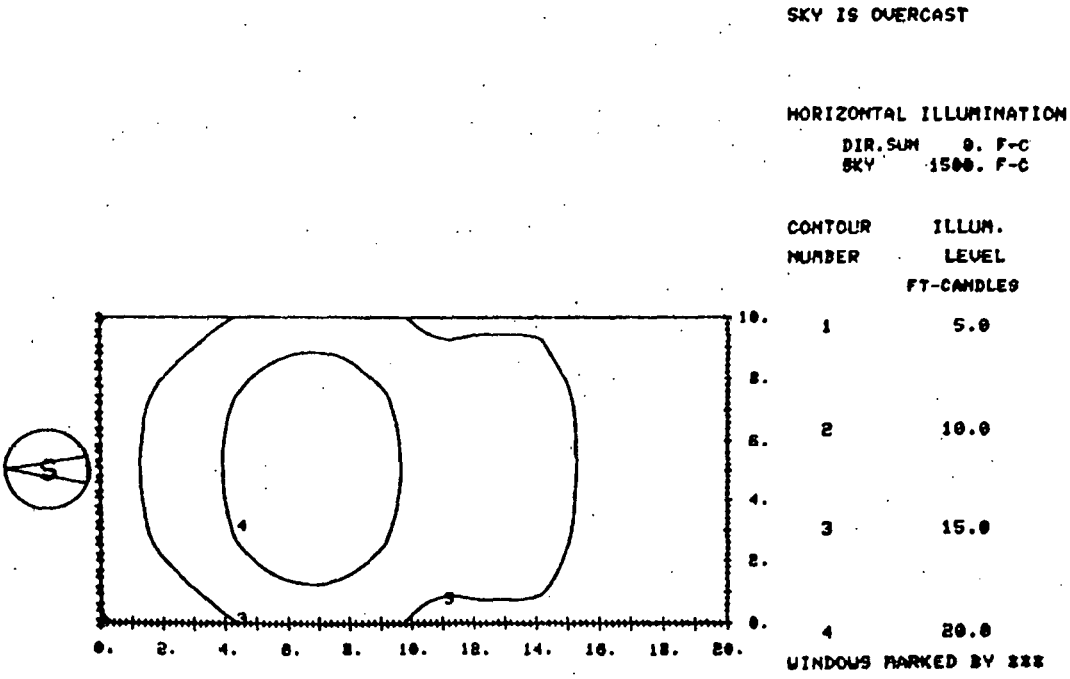

Figure 15: Illumination Levels in a Rectangular Room on an Overcast Day With Light Shelf (ρ= 0.9)

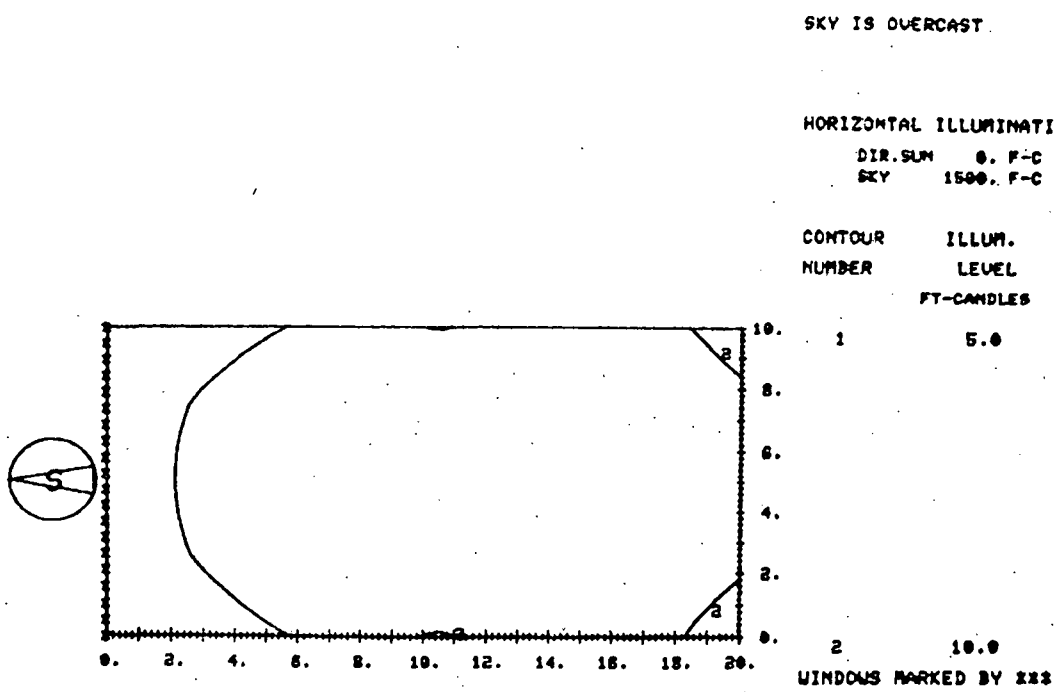

Figure 16: Illumination Levels in a Rectangular Room on an Overcast Day With Light Shelf (ρ= 0.2)

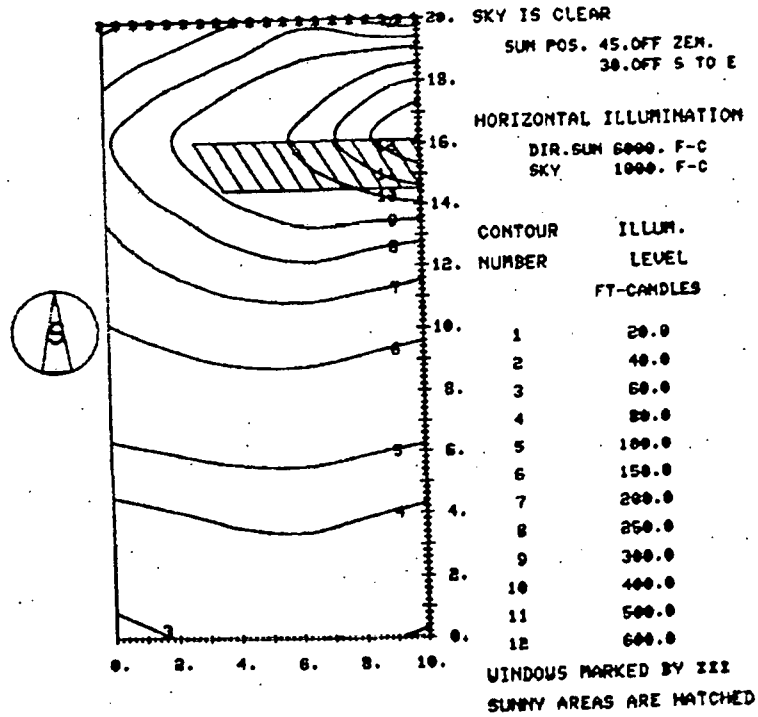

Figure 17: Illumination Levels in a Rectangular Room on a Clear Day Without Light Shelf

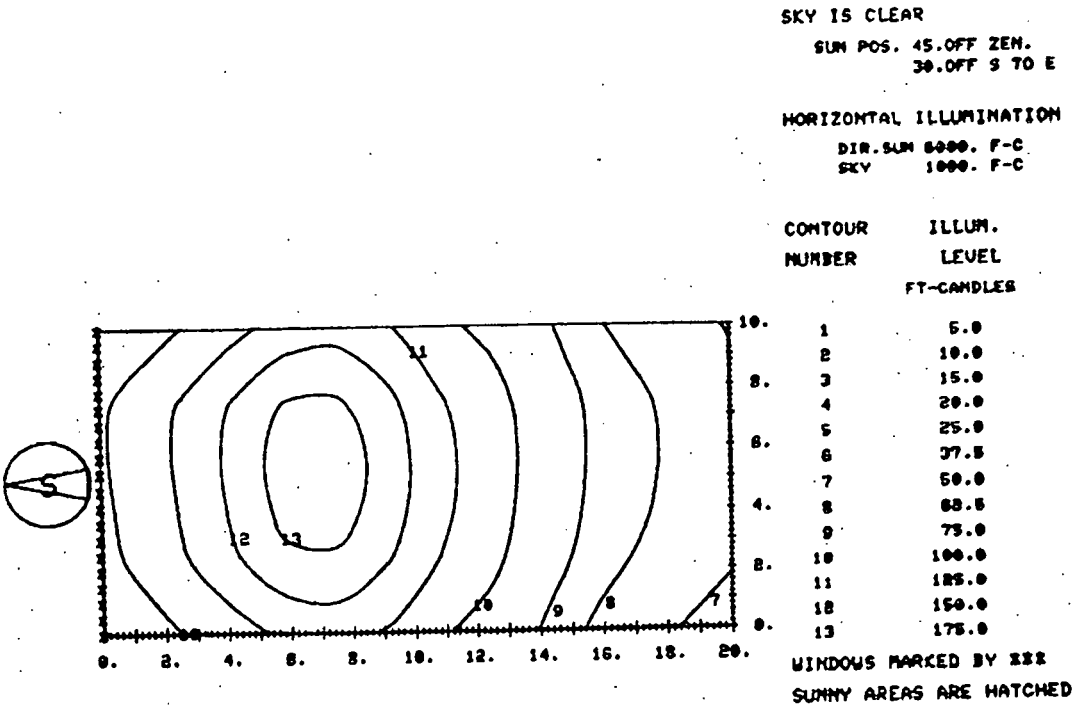

Figure 18: Illumination Levels in a Rectangular Room on a Clear Day with Light Shelf (ρ = 0.9)

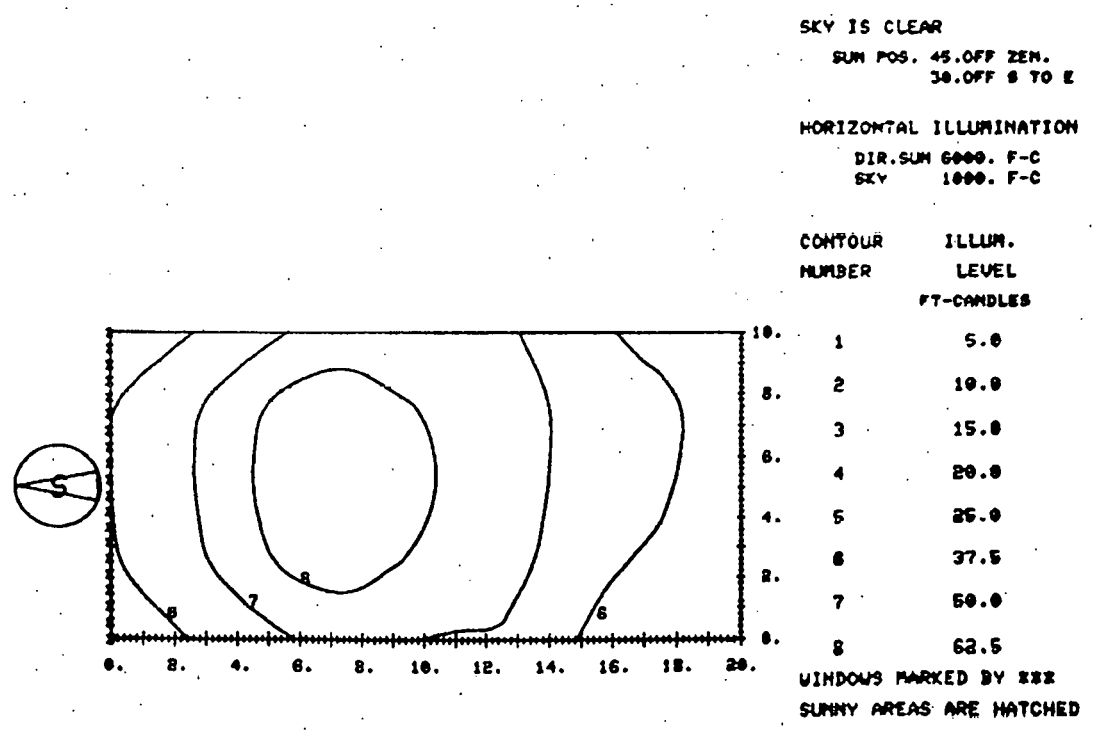

Figure 19: Illumination Levels in a Rectangular Room on a Clear Day with Light Shelf (ρ = 0.2)

TECHNICAL INFORMATION DEPARTMENT
LAWRENCE BERKELEY LABORATORY
UNIVERSITY OF CALIFORNIA
BERKELEY, CALIFORNIA 94720